

ON THE EFFECTIVENESS OF DOUBLY ADAPTIVE ESTIMATION FOR DYNAMIC MRI SEQUENCE ACQUISITIONS

W. Scott Hoge*, Lawrence P. Panych

Brigham and Women's Hospital
and Harvard Medical School
Department of Radiology
75 Francis Street, Boston, MA 02115

Dana H. Brooks, Eric L. Miller,
and Hanoch Lev-Ari

Northeastern University
ECE Department
360 Huntington Ave., Boston, MA 02115

ABSTRACT

We present experimentally-acquired MR image sequence reconstruction results and a review of the recently proposed *doubly adaptive temporal update method* (DATUM) for the acquisition of dynamic MRI sequences. The DATUM algorithm is novel in providing an estimation and tracking framework for both image reconstruction and the image acquisition inputs.

We discuss the difficulty in choosing viable system inputs adaptively and compare DATUM to other minimal data MRI acquisition techniques. New results of image estimates constructed from data acquired on a standard production MRI scanner show that adapting system inputs to the sequence provides substantial image quality improvement to dynamic sequence estimation.

1. INTRODUCTION

While the clinical use of magnetic resonance imaging (MRI) is widespread today, physicians continue to push for better temporal and spatial resolution in dynamic MR image sequences. Historically, there have been two complementary approaches to meeting this need. One approach is to enhance the physical hardware, for example by using an array of coils to improve temporal resolution. The complementary approach is to develop algorithms which exploit the data redundancy in standard MRI data acquisition methods.

Central to the algorithmic approach of dynamic sequence acquisition are the two issues of *image estimation* and *input selection*. Previous algorithmic approaches have concentrated primarily on image estimation utilizing a static set of data acquisition inputs. Building on this approach, our group recently presented the theoretical fundamentals for a new MRI data acquisition algorithm [1] that provides a

*Research supported by NIH NRSA Training Grant PA-00-103, and CenSSIS (the Center for Subsurface Sensing and Imaging Systems) under the Engineering Research Centers Program of the National Science Foundation (Award Number EEC-9986821).

mechanism to adaptively determine both the image estimate and an appropriate set of inputs in tandem. By dynamically varying the inputs for each acquired image in the sequence, very high quality estimates of the dynamic sequence can be achieved.

We present here a brief description of the DATUM method, a discussion on the difficulty of choosing new input from previous estimates, and results acquired on a standard production MRI scanner.

2. PROBLEM FORMULATION

The DATUM method builds on the linear MRI acquisition system model described by Panych, et. al., in [2]. Under the assumption of low tip angles and rf encoding, the data acquisition process can be described as a matrix-vector product

$$Y_n = A_n X_n \quad (1)$$

where the columns of X_n and Y_n represent samples of the input and output rf waveforms, respectively, and A_n represents data for a single image slice at a given time n . For many image acquisition protocols, the acquisition time is proportional to the number of inputs used. Thus for minimal data acquisition and reconstruction, X_n and Y_n should be tall-thin matrices with r columns. For an image data matrix of size $M \times N$, X_n and Y_n are of size $N \times r$ and $M \times r$ respectively. We choose to restrict the columns of the input matrix X_n to be orthonormal, both to follow historical precedent and because it greatly simplifies the analysis.

Due to the fundamental principles of MRI data acquisition, A_n is typically the frequency encoded, or k -space, representation of the image data. To view the image, this data can be transformed to the spatial domain through appropriate use of the unitary Fourier transform matrix [3, Chp. 5].

2.1. Image Estimation

Our approach to image reconstruction is to cast the problem in a minimization framework. Ideally, we would like to minimize the difference between our image estimate and the true image:

$$\mathcal{E}_n = \|A_n - \hat{A}_n\|_F^2. \quad (2)$$

However, we only have access to the image data through the input/output system model (1). Thus, we instead construct an image estimate that minimizes the difference between the expected output $\hat{Y}_n = \hat{A}_n X_n$ and the actual output Y_n , via

$$\min_{\hat{A}_n} \mathcal{J}_n = \|Y_n - \hat{A}_n X_n\|_F^2. \quad (3)$$

This minimization problem is underdetermined, and an infinite number of solutions exist. Different image reconstruction techniques can be found by applying different models for the image estimate. For example, a direct solution of (3) leads to a *low rank* reconstruction, which was used in the first SVD paper by Zientara, et. al. [4]

$$\hat{A}_n = Y_n X_n^H. \quad (4)$$

Alternatively, modeling the estimate as a reference image, A_{ref} , plus a change, leads to a data replacement reconstruction, as described in the Fourier Keyhole (FK) method of van Vaals, et. al. [5].

$$\hat{A}_n = Y_n X_n^H + A_{\text{ref}}(I - X_n X_n^H). \quad (5)$$

Finally, the image estimate can be modeled as a change from a previous estimate. This leads to an adaptive filter style reconstruction

$$\hat{A}_n = Y_n X_n^H + \hat{A}_{n-1}(I - X_n X_n^H). \quad (6)$$

The quality of each of these image estimates is assessed via the original estimate error measure given in (2). In addition, (2) can provide a useful guide for the choice of subspace inputs as shown below.

2.2. Input Selection

The estimate error, (2), for each of the reconstruction methods above is given in Table 1. Clearly, for each reconstruction method, the image estimate error at time n is directly dependent on the choice of inputs at time n . This implies that if one knew which inputs to use, image sequence acquisitions utilizing dynamic inputs would likely be of higher quality than static inputs.

In each case, the estimate error is characterized by an image (or image difference) matrix operated on the right by a subspace projection operator, assuming orthonormal inputs. If the sequence were completely known, then Table 1

Method	Eq.	Estimate Error
Low-rank	(4)	$\mathcal{E}_n = \ A_n(I - X_n X_n^H)\ _F^2$
Keyhole	(5)	$\mathcal{E}_n = \ (A_n - A_{\text{ref}})(I - X_n X_n^H)\ _F^2$
Adaptive	(6)	$\mathcal{E}_n = \ (A_n - \hat{A}_{n-1})(I - X_n X_n^H)\ _F^2$

Table 1. Summary of the image estimate error, \mathcal{E}_n , for the low-rank, keyhole, and adaptive framework methods.

could be used to identify the *theoretically optimal* inputs at time n for a given reconstruction method. Thus, we find that the inputs to minimize \mathcal{E}_n are: (a) the r dominant right singular vectors (rSV) of the next image for the low-rank estimate method (4); (b) the rSV of the difference between the next image and reference image for the Keyhole method (5); and (c) the rSV of the difference between the next image and current estimate for the adaptive estimate method (6).

Of course in a clinical setting the next image is not available, so must it must be estimated as well. These estimates can be obtained via image prediction and used to determine an appropriate set of image acquisition inputs for the next image in a sequence. Choices for a suitable predictor are discussed in the following section.

2.3. The Subspace Trap

While high quality image prediction is desirable for accurately driving the system input selection, it is in fact not necessarily required. Considering the results of Table 1, the true goal is to select the proper acquisition input subspace — and a wide variety of image predicting methods in fact will lead to a poor input vector selection via a process we term the *subspace trap*.

The clearest example of the subspace trap is visible if one uses the low-rank reconstruction, $\hat{A}_n = Y_n X_n^H = A_n X_n X_n^H$. The subspace projection on the right indicates that the right singular vectors of this estimate will always span the basis supported by the input vector matrix X_n used to acquire the image. Thus, utilizing only the rSV of the current estimate to choose new inputs is no better than maintaining static inputs.

A similar conclusion is reached when using a keyhole style reconstruction, $\hat{A}_n = A_n X_n X_n^H + A_{\text{ref}}(I - X_n X_n^H)$. In this case the signal power in the residual part of the reference image will likely be orders of magnitude less than the most recent low rank reconstruction contribution of the estimate. This is particularly true for the case when X_n captures either the low frequencies of k -space, as in the FK method, or is derived from the rSV of A_{ref} . Thus, one can expect that new input vectors chosen from the rSV of \hat{A}_n will again be biased towards the subspace spanned by $X_n X_n^H$.

Finally, for the adaptive method, the first impulse is to use a predictor based on the full rank estimate. However,

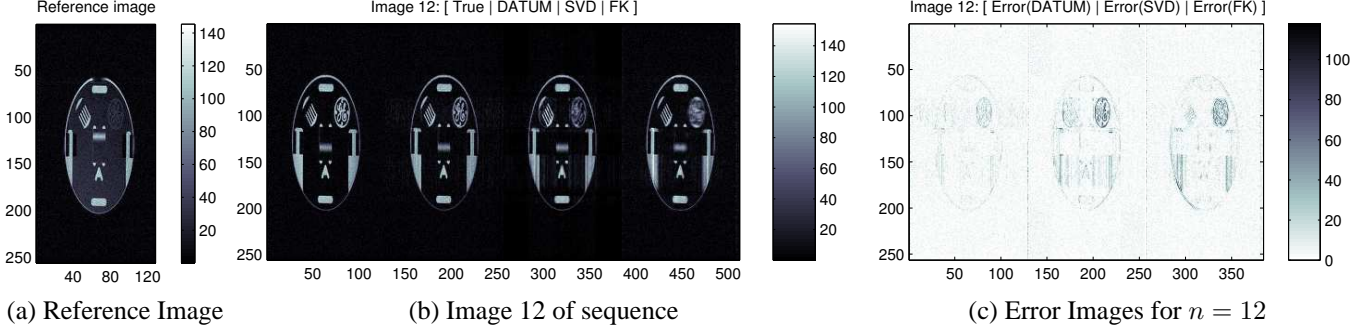


Fig. 1. Images from a synthesized dynamic GE phantom acquisition sequence. (a) The first image in the sequence, which is the reference image for the static input methods (SVD and FK). (b) Estimates of Image 12 in the sequence. From left to right the reconstructions are: the entire k -space data set (i.e. the True Image), the DATUM estimate, the SVD estimate, and the FK estimate. (c) Absolute error images for Image 12. From left to right, the error images are: $|(A_{\text{True}} - \hat{A}_{\text{DATUM}})|$, $|(A_{\text{True}} - \hat{A}_{\text{SVD}})|$, and $|(A_{\text{True}} - \hat{A}_{\text{FK}})|$.

consider the case of predicting the next image from two previous image estimates using linear temporal prediction. With the predictor inputs denoted \check{A}_n , this predictor is

$$\tilde{A}_{n+1} = \check{A}_n + (\check{A}_n - \check{A}_{n-1}).$$

For the case when the predictor input is the adaptive-style estimate of (6) we find

$$\begin{aligned} (\tilde{A}_{n+1} - \hat{A}_n) &= (2\hat{A}_n - \hat{A}_{n-1}) - \hat{A}_n = \hat{A}_n - \hat{A}_{n-1} \\ &= (A_n - \hat{A}_{n-1})X_nX_n^H. \end{aligned} \quad (7)$$

Again, the expression $X_nX_n^H$ indicates a subspace projection. Thus, the dominant right singular vectors of $(\tilde{A}_{n+1} - \hat{A}_n)$ will span the same subspace as X_n , and input vectors chosen via this approach will span the same subspace at every time n — a subspace trap.

A better choice with this predictor is to use the low rank reconstruction as the input, i.e. $\check{A}_n = Y_nX_n^H$. In this case we find

$$\begin{aligned} (\tilde{A}_{n+1} - \hat{A}_n) &= (2Y_nX_n^H - Y_{n-1}X_{n-1}^H) - \hat{A}_n \\ &= A_nX_nX_n^H - A_{n-1}X_{n-1}X_{n-1}^H + \\ &\quad \hat{A}_{n-1}(I - X_nX_n^H). \end{aligned} \quad (8)$$

In this case, the right singular vectors of $(\tilde{A}_{n+1} - \hat{A}_n)$ will not necessarily be biased towards X_n . The results shown in the next section demonstrate that high quality image sequence estimates can be found using a simple linear predictor using low-rank reconstruction estimates as inputs.

3. EXPERIMENTAL RESULTS

The results presented here show a comparison between the DATUM, Fourier Keyhole (FK) and SVD methods. The primary difference between these methods is that the image

acquisition inputs are recalculated for each new image under the DATUM acquisition, whereas they are static for the other two methods.

The dynamic image sequences were acquired on a GE 1.5T Signa LX scanner using a spin echo pulse sequence modified to perform rf encoding in place of phase encoding. To synthesize changes in the field of view (FOV), each image in the series was acquired at a different position along the axial direction of the phantom. $r = 32$ input vectors were used for each minimal data image acquisition. Compared to the 128 input vectors needed to obtain the entire true image k -space data set, this gives an effective acquisition time ratio of 1:4. This implies a $4\times$ increase in the temporal resolution of the sequence using the minimal data acquisition methods.

The DATUM reconstructions used (6) for the image estimates and new inputs were determined from the 32 dominant right singular vectors (rSV) of $(\tilde{A}_{n+1} - \hat{A}_n)$ using a simple three point linear interpolation predictor:

$$\tilde{A}_{n+1} = [4Y_nX_n^H + 3Y_{n-1}X_{n-1}^H - 2Y_{n-2}X_{n-2}^H]/3. \quad (9)$$

Comparatively, the FK method acquires the low frequency components of k -space for each new image, using (5) for the image reconstruction. The SVD method acquires a subset of the image data projected onto the subspace corresponding to the rSV of the first image in the sequence and uses (4) for the image reconstruction.

Images from a dynamic sequence acquisition using the minimal data acquisition methods are shown in Figs. 1 and 2. Using a common GE phantom, each slice of the sequence was 3mm thick with a 1mm step size between each slice. The imaging protocol parameters were: TR = 500 msec; TE = 14 msec. Fig. 1(a) shows the first image in the sequence, which was used as the reference image for the FK and SVD methods. The notable changes that occur in this sequence are a gradual intensity change of the GE logo in the upper

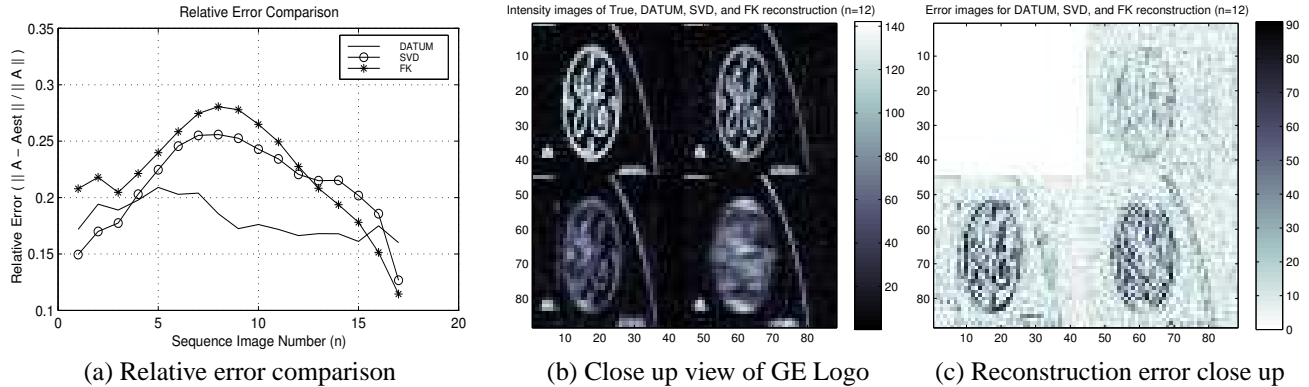


Fig. 2. Comparison of dynamic GE phantom sequence estimates. (a) Relative error comparison for each of the minimal data acquisition methods. (b) Close up view of GE logo for Image 12. Clockwise starting at the upper left: True Image, DATUM estimate, FK estimate, SVD estimate. (c) Close up view of estimation error in GE logo for Image 12. Clockwise starting at the upper right: DATUM estimate error, FK estimate error, SVD estimate error.

right corner, a widening of the vertical bars on either side of the phantom, and a lowering of the center bar.

Fig. 1(b) shows the twelfth image in the sequence and compares each of the three minimal data acquisition methods to the true full k -space image. Clearly, from the absolute value of the image estimate error for each method shown in Fig. 1(c), there is significantly less error in the DATUM estimate than either of the static input methods (SVD and FK).

The quality of the DATUM method estimate is consistent throughout the sequence, as shown in Fig. 2(a) which compares the relative pixel error for each method at each image estimate. The relative error is defined as $re(\hat{A}_n, A_n) = \|A_n - \hat{A}_n\|_F^2 / \|A_n\|_F^2$. Due to the phantom construction, the last image in the sequence becomes a full circle with no structure detail. Thus the FK method is expected to outperform the non-Fourier methods in this case. However, this dramatic structural change does not reflect scenarios where DATUM estimation is anticipated to be applied. Thus, the “recovery” of the FK method in this plot is immaterial.

A close-up view of the estimates at $n = 12$ is given in Fig. 2(b). This view shows that the DATUM method accurately reconstructs the detail in the GE logo, lacking only in the intensity level of the image. In contrast, the SVD and FK methods show a significant amount of blurring in the image estimate. The DATUM estimate quality is further confirmed by Fig. 2(c) which shows that the error is distributed across the FOV in the DATUM estimate, whereas it is concentrated on the edges of the structural detail in the SVD and FK estimates.

4. CONCLUSION

This abstract presented new image reconstructions from a dynamic sequence acquired on a standard MRI scanner. These images support the claim that dynamically varied

inputs derived from the *doubly adaptive temporal update method* (DATUM) can produce image sequence estimates of higher quality than static input minimal data acquisition methods. In addition, we discussed some of the subtleties of choosing new image acquisition input vectors from previous estimates, which is central to DATUM estimation.

Current and future research in this area is focused on more sophisticated image predictor methods. It is anticipated that better image prediction will be able to better guide the input selection process, resulting in even better image sequence estimation.

5. REFERENCES

- [1] W. S. Hoge, E. L. Miller, and et. al., “Doubly adaptive estimation of dynamic MRI sequences,” in *Proc. ISMRM Minimum MR Data Acquisition Methods Workshop (Marco Island, FL)*, Oct. 2001, pp. 98–101.
- [2] L. P. Panych, G. P. Zientara, and F. A. Jolesz, “MR image encoding by spatially selective rf excitation: An analysis using linear response models,” *Int. J. Imaging Syst. Technol.*, vol. 10, no. 2, pp. 143–150, 1999.
- [3] A. K. Jain, *Fundamentals of Digital Image Processing*, Information and System Sciences. Prentice Hall, 1989.
- [4] G. P. Zientara, L. P. Panych, and F. A. Jolesz, “Dynamically adaptive MRI with encoding by singular value decomposition,” *Magn. Reson. in Med.*, vol. 32, pp. 268–274, 1994.
- [5] J. van Vaals, M. E. Brummer, and et. al., “Keyhole method for accelerating imaging of a contrast agent uptake,” *J. of Magn. Reson. Imag.*, vol. 3, no. 4, pp. 671–675, 1993.